Centromere repositioning causes inversion of meiosis and generates a reproductive barrier

Min Lu[a] and Xiangwei He[a,1]

[a]Ministry of Education Key Laboratory of Biosystems Homeostasis & Protection and Innovation Center for Cell Signaling Network, Life Sciences Institute, Zhejiang University, 310058 Hangzhou, Zhejiang, China

Edited by J. Richard McIntosh, University of Colorado, Boulder, CO, and approved September 20, 2019 (received for review July 10, 2019)

The chromosomal position of each centromere is determined epigenetically and is highly stable, whereas incremental cases have supported the occurrence of centromere repositioning on an evolutionary time scale (evolutionary new centromeres, ENCs), which is thought to be important in speciation. The mechanisms underlying the high stability of centromeres and its functional significance largely remain an enigma. Here, in the fission yeast *Schizosaccharomyces pombe*, we identify a feedback mechanism: The kinetochore, whose assembly is guided by the centromere, in turn, enforces centromere stability. Upon going through meiosis, specific inner kinetochore mutations induce centromere repositioning—inactivation of the original centromere and formation of a new centromere elsewhere—in 1 of the 3 chromosomes at random. Repositioned centromeres reside asymmetrically in the pericentromeric regions and cells carrying them are competent in mitosis and homozygotic meiosis. However, when cells carrying a repositioned centromere are crossed with those carrying the original centromere, the progeny suffer severe lethality due to defects in meiotic chromosome segregation. Thus, repositioned centromeres constitute a reproductive barrier that could initiate genetic divergence between 2 populations with mismatched centromeres, documenting a functional role of ENCs in speciation. Surprisingly, homozygotic repositioned centromeres tend to undergo meiosis in an inverted order—that is, sister chromatids segregate first, and homologous chromosomes separate second—whereas the original centromeres on other chromosomes in the same cell undergo meiosis in the canonical order, revealing hidden flexibility in the perceived rigid process of meiosis.

inner kinetochore | CENP-T-W-S-X complex | centromere repositioning | reproductive barrier | inverted meiosis

Centromeres dictate the sites on chromosomes for kinetochore assembly and provide the foundation for spindle microtubule attachment to assure the faithful chromosome transmission during mitosis and meiosis (1, 2). For most eukaryotes, including humans and fission yeast, centromeres span a specific region—tens of kilobases in the fission yeast *Schizosaccharomyces pombe*, up to megabases in mammals and plants—of the chromatin, which are called monocentromeres. The position of the centromere on each chromosome is determined epigenetically by an evolutionarily conserved histone H3 variant, CENP-A (3). While the underlying centromeric DNA sequences are usually highly repetitive (called satellite or alphoid DNA), they diverge dramatically among species. Furthermore, the underlying DNA sequence does not determine the site of a centromere. The formation of a functional neocentromere, defined by a new centromere formed on an ectopic site other than that of the original centromere, is independent of the DNA sequence (4).

Centromere positioning on each chromosome is remarkably stable in all eukaryotes, although centromere repositioning due to neocentromere formation without alteration in the chromosomal marker order does occur sporadically in contemporary populations (e.g., 8 cases have been reported in humans) (5) and among related species (such as primates) on the evolutionary time scale (i.e., evolutionary new centromeres, ENCs) (6). It is postulated that a neocentromere may seed the formation of an ENC at a site devoid of satellite DNA, which is then matured through acquisition of repetitive DNA. ENCs and neocentromeres are considered as two sides of the same coin, manifestations of the same biological phenomenon at drastically different time scales and population sizes (7). Hence, understanding centromere repositioning may provide mechanistic insights into ENC emergence and progression.

CENP-A–containing chromatin directly recruits specific components of the kinetochore, called the constitutive centromere-associated network. The kinetochore is a proteinaceous machinery comprised of inner and outer parts, each compassing several subcomplexes. The inner kinetochore is proximal to or in direct contact with the CENP-A nucleosomes, linking the centromere to the outer kinetochore, which in turn physically binds the spindle microtubules (8). Mutations in the N-terminal tail of CENP-A reduce the centromeric localization of the inner kinetochore component CENP-T and cause centromere inactivation (9). Previous studies, including ours (10), have shown that kinetochore components may contribute to the stability of the centromeric chromatin organization pattern. Certain inner kinetochore components (e.g., Mis6 and Cnp3 in *S. pombe*; CENP-C and CENP-N in vertebrates) are required for maintaining proper levels of CENP-A nucleosomes in centromeres (11–14). Moreover, partial dysfunction of the kinetochore (e.g., *mis6-302*, *mis12-537*, and *ams2Δ*) facilitates centromere inactivation and rescues the high rates of lethality caused by an engineered dicentric

Significance

Mutations in inner kinetochore components induce centromere repositioning without alteration in the centromeric DNA sequence, revealing a feedback mechanism underlying the high epigenetic stability of the centromere. This also provides a desirable experimental system to explore the functional significance of centromere positioning in meiosis. We discovered that in a heterozygotic meiosis, a repositioned centromere generates a reproductive barrier, suggesting a functional role of evolutionary new centromeres in speciation; furthermore, in a homozygotic meiosis, chromosomes carrying repositioned centromeres frequently undergo the 2 stages of meiotic segregation in an inverted order, demonstrating high flexibility in the meiotic process.

Author contributions: M.L. conceived the project; M.L. and X.H. designed research; M.L. performed research; M.L. analyzed data and prepared figures; and M.L. and X.H. wrote the paper.

The authors declare no competing interest.

This article is a PNAS Direct Submission.

Data deposition: The data reported in this paper have been deposited in the Gene Expression Omnibus (GEO) database, https://www.ncbi.nlm.nih.gov/geo (accession no. GSE118016).

[1]To whom correspondence may be addressed. Email: xhe@zju.edu.cn.

This article contains supporting information online at www.pnas.org/lookup/suppl/doi:10.1073/pnas.1911745116/-/DCSupplemental.

First published October 9, 2019.

chromosome in fission yeast (15). In general, these data suggest functional cross-talk between the centromere and the kinetochore.

Centromere–kinetochore–microtubule attachment is crucial for accurate chromosome segregation in mitosis as well as meiosis. Meiosis occurs in eukaryotes that generate germ cells for sexual reproduction. Canonical meiosis involves 2 sequential nuclear divisions (meiosis I and meiosis II) following 1 round of DNA replication (16). The order of the segregation events is highly conserved. It is characterized by homologous chromosome pair separation during the first "reductional" division (meiosis I) followed by sister chromatids segregation during the second "equational" division (meiosis II). To accomplish faithful chromosome segregation in such a distinct manner, sister kinetochores must initially establish connection with only 1 pole of the spindle in meiosis I (called "mono-orientation") so that they are cosegregated, whereas in meiosis II, they must establish biorientation with the 2 poles of the spindle in order to be segregated equally. In addition, crossover and sequential resolution of chromosome cohesion along chromosome arms in meiosis I and at centromeres in meiosis II are also necessary to fulfill the requirements of the specific order of meiotic nuclear divisions (17).

Interestingly, despite the common perception of the strict order of 2 nuclear divisions in canonical meiosis, inverted order of meiotic divisions (inverted meiosis) has been discovered in a few species with holocentromeres in which centromeres are distributed throughout the chromosomes, and is considered as one of several strategies specifically adopted by the holocentric organisms for meiosis (18–21). Surprisingly, a recent study in human female germline cells demonstrated that inverted meiosis also occurs in a monocentric organism (22). We here investigate in fission yeast how kinetochore mutations may affect centromere stability and report the functional consequences of repositioned centromeres in generating a reproductive barrier and inversion in the order of segregation events in meiosis.

Results

Inner Kinetochore Mutations Cause Various Levels of Pericentromeric Heterochromatin Spreading into Centromeric Core Regions. Fission yeast haploid cells possess 3 chromosomes and exhibit a characteristic centromeric chromatin organization pattern (23). The central cores, consisting of mostly unique DNA sequences (*cnt*) and part of the innermost repeats (*imr*), are occupied by Cnp1/CENP-A nucleosomes interspersed with canonical H3 nucleosomes, whereas the flanking regions comprising repetitive DNA sequences (outermost repeats *otr* and part of *imr*) are packed into heterochromatin (24, 25), as marked by histone H3 lysine 9 methylation (H3K9me2) (26). The boundaries between the heterochromatin and the central cores are strictly delimited by *tDNA* elements (Fig. 1, diagrams) (27). We sought to investigate the mechanisms underlying the epigenetic stability of this centromeric chromatin organization.

We hypothesized that the kinetochore may inversely affect the centromere. To test this, we systematically investigated the impact of kinetochore mutations on centromeric chromatin organization. Anti-H3K9me2 chromatin immunoprecipitation and high-throughput sequencing (ChIP-seq) were performed in mutants with either deletions of nonessential kinetochore component genes or conditional inactivation (temperature sensitive) mutations in the essential ones. These genes encode representative components of all inner and some outer kinetochore subcomplexes (8). Pericentromeric heterochromatin spreading into the core regions to various degrees was detected: Whereas the outer kinetochore mutants (*nuf2-1* and *mis12-537*) showed no heterochromatin spreading, the inner kinetochore mutants (*mis15-68*, *sim4-193*, *mal2-1*, *fta6Δ*, and *cnp3Δ*) exhibited minor to major levels of heterochromatin encroaching into the core regions in 1 or 2 centromeres (Fig. 1*A* and *SI Appendix*, Fig. S1*A*). Noticeably, temperature-sensitive strains, for example *sim4-193*, displayed a similar heterochromatin spreading at the nonpermissive and permissive temperatures, indicating that centromeric chromatin organization is already impaired in cells under the viable condition. *mhf2Δ* (mammalian CENP-X homolog) exhibited complete heterochromatin occupancy in one centromere (*cen1*) but normal pericentromeric distribution in the other two (*cen2* and *cen3*) (Fig. 1*A* and *SI Appendix*, Fig. S1*A*). The island-shape ChIP-seq signals detected on *cnt3* in *mhf2Δ* are most likely caused by an artifact in informatics data processing as the border of the small island aligns precisely with the identical sequence in *cnt1* and *cnt3*, which is biochemically highly unlikely (also see below). In a double-mutant *cnp3Δfta6Δ* strain, derived from genetic crossings, we found that *cen2* was completely covered by heterochromatin (Fig. 1*A* and *SI Appendix*, Fig. S1*A*), suggesting that perturbations to centromeric chromatin by *cnp3Δ* and *fta6Δ* cumulatively led to centromere inactivation.

Anti-Cnp1 ChIP-seq detected no significant Cnp1 signal at centromeric cores occupied by heterochromatin but prominent levels of Cnp1 at the other two in both *mhf2Δ* and *cnp3Δfta6Δ* (Fig. 1*B*), confirming that only the original *cen1* or *cen2* was inactivated (designated as $cen1^{inactive}$ and $cen2^{inactive}$ hereafter) in these 2 strains, respectively. Due to the possible informatics artifact of the "island-shape" signals in the inactivated *cen1* in *mhf2Δ*, we cannot formally exclude the possibility that some Cnp1 persists there. However, the complete removal of Cnp1 occupancy and the fully coverage of H3K9me2 on the inactivated *cen2* in *cnp3Δfta6Δ* are in favor of the scenario that the inactivated centromeres do not contain Cnp1. Taken together, these results demonstrate that the integrity of the inner kinetochore is required to maintain normal centromeric chromatin organization as well as distinct centromere identity. The effects appear specific to these mutants as we also examined mutants of genes encoding other centromere-interacting proteins known to affect centromeric Cnp1 incorporation, but detected no noticeable (*mis16-53*, *mis18-262*) or only minor (*ams2Δ* and *sim3Δ*) heterochromatin spreading (*SI Appendix*, Fig. S1*B*) (28–30).

Single Depletion of CENP-T-W-S-X Components Induces Centromere Inactivation. CENP-T-W-S-X is a conserved inner kinetochore complex in which each subunit contains a histone-fold domain that binds directly to DNA (31). To further explore the role of the CENP-T-W-S-X complex in maintaining centromere identity, we generated heterozygous deletion diploid strains de novo for the 3 nonessential components: *wip1*/CENP-W, *mhf1*/CENP-S, and *mhf2*/CENP-X (*cnp20*/CENP-T is essential for cell viability and is not included in this study) (12). Tetrad analysis of the meiotic progeny of each strain showed that most of the asci contained only two or fewer viable spores, demonstrating a significant reduction in meiotic progeny viability. However, the lethality was similar between the wild-type and mutant haploid progeny (*SI Appendix*, Table S1). Furthermore, among the surviving progeny, anti-Cnp1 ChIP-seq detected random inactivation in only 1 of the 3 centromeres in each of the 10 tested *wip1Δ*, *mhf1Δ*, or *mhf2Δ* haploid strains (Fig. 2 *A* and *C* and *SI Appendix*, Fig. S3*A* and Table S2), whereas the wild-type progeny from the same asci exhibited no heterochromatin occupancy in the centromeric cores by anti-H3K9me2 ChIP-seq but Cnp1 spreading into the pericentromeric regions by anti-Cnp1 ChIP-seq (Fig. 2*B* and *SI Appendix*, Fig. S3 *B* and *C*). Hence, centromere inactivation is tightly linked with the gene deletions. Centromere inactivation was not observed in the parental heterozygous deletion diploid cells (Fig. 2*B*), excluding the possibility that centromere inactivation occurred premeiotically. No haploid deletion strain was found carrying more than 1 inactivated centromere. We speculate that simultaneous inactivation of 2 or 3 centromeres may be incompatible with cell survival. In a few (6.1%) *mhf2Δ*/+ asci containing 4 viable spores, the *mhf2Δ* progeny grew slower than the wild-type, formed minicolonies but frequently gained a growth

CELL BIOLOGY

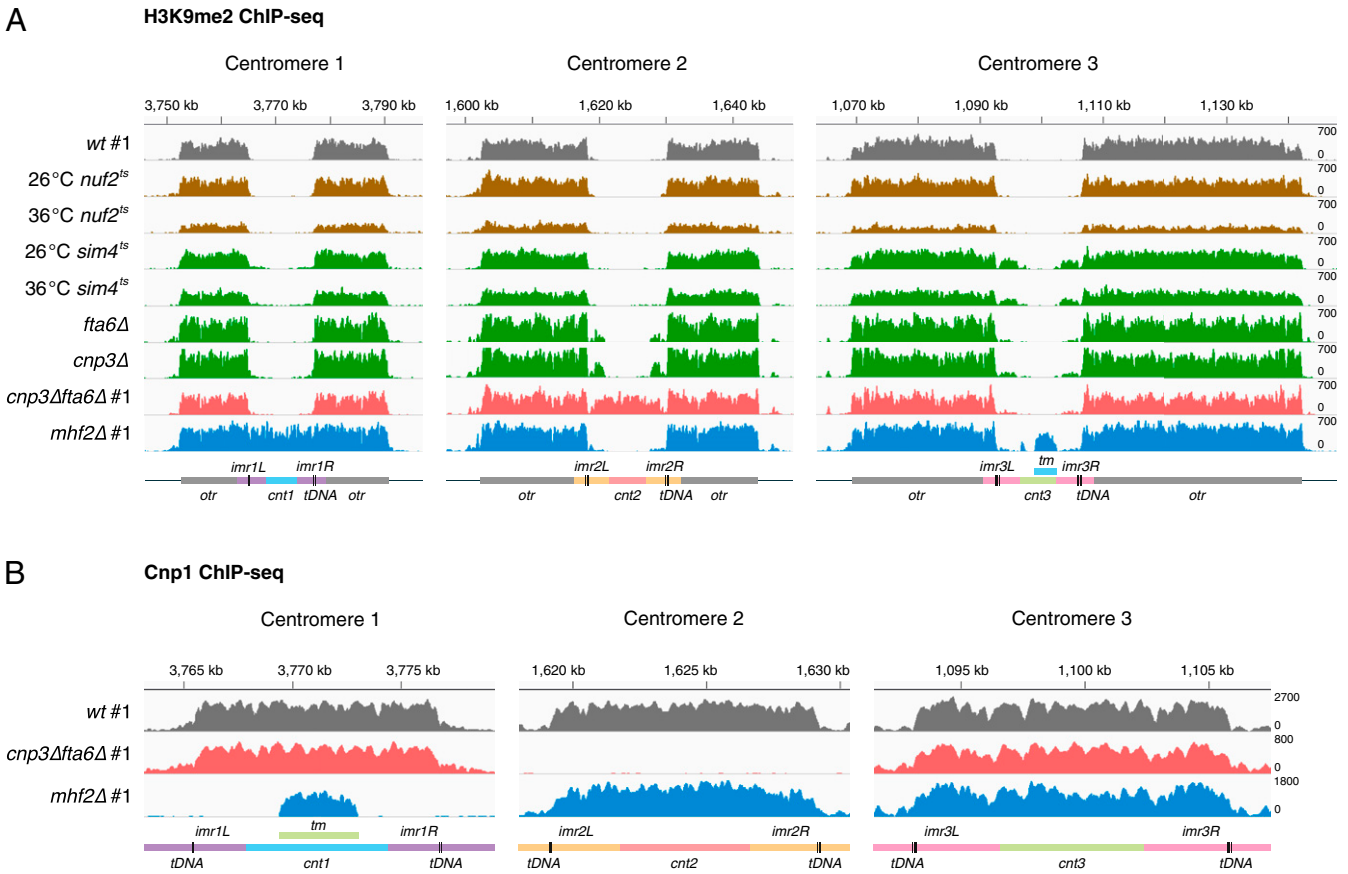

Fig. 1. Inner kinetochore mutations cause various levels of pericentromeric heterochromatin spreading into centromeric core regions. (*A*) H3K9me2 ChIP-seq reads mapped to centromeric and pericentromeric regions of all 3 chromosomes in outer kinetochore mutants (brown), inner kinetochore mutants (green), *mhf2Δ* (blue), and *cnp3Δfta6Δ* (pink) compared to wild-type cells (gray). Strain names are as labeled. *mhf2Δ* (blue) and *cnp3Δfta6Δ* (pink) show complete occupancy of H3K9me2 on *cnt1* and *cnt2*, respectively. Temperature sensitive (ts) strains were incubated at 26 °C (labeled as 26 °C), or incubated at 26 °C and shifted to 36 °C for 6 h (labeled as 36 °C). (*B*) Cnp1 ChIP-seq reads mapped to centromeric regions of all 3 chromosomes in *mhf2Δ* (blue) and *cnp3Δfta6Δ* (pink) compared to wild-type cells (gray). Tested strains were identical to that used in H3K9me2 ChIP-seq analysis as labeled in *A*. #1, Biological replicate 1. Diagrams illustrate the organization of centromeres 1, 2, and 3. *tDNA*, vertical lines; tm, segments with identical sequences in *cnt1* and *cnt3*. The *x* axis, DNA coordinates on chromosomes 1, 2, and 3 according to reference genome (pombase.org); *y* axis, reads per million of ChIP-seq reads randomly assigned to the repetitive DNA sequences. The wild-type ChIP-seq raw data were previously published (10).

advantage after restreaking several times (*SI Appendix*, Fig. S2). Among them, 2 *mhf2Δ* progeny carrying different inactivated centromeres (*cen2*$^{\text{inactive}}$ and *cen3*$^{\text{inactive}}$, respectively) were recovered from the same ascus, further supporting the notion that centromere inactivation occurred postzygotically and independently in each progeny (Fig. 2*C*).

Neocentromeres Are Formed Preferentially in the Pericentromeric Regions. A previous study in fission yeast has shown that with complete excision of *cen1* DNA by genome editing, a few cells (less than 0.1%) survive by either forming a neocentromere at a new location or fusing the acentric chromosome to another chromosome (32). To determine whether the surviving *mhf2Δ* cells acquired neocentromeres, we microscopically examined *mhf2Δcen1*$^{\text{inacitve}}$ cells expressing a green fluorescent protein-tagged outer kinetochore protein Ndc80-GFP for the presence of a complete set of kinetochores (3 pairs of sister kinetochores). Six discrete dots were resolved in a few M phase cells with sufficiently scattered kinetochores (Fig. 3*A*), suggesting that a functional kinetochore (and thereby, a neocentromere) was formed on chromosome 1 carrying *cen1*$^{\text{inacitve}}$.

To determine the locations of neocentromeres, anti-Cnp1 ChIP-seq was performed in *mhf2Δcen1*$^{\text{inactive}}$ and *mhf2Δcen2*$^{\text{inactive}}$. While prominent levels of Cnp1 were present in the other 2 active and original centromeres, modest but clearly detectable Cnp1 appeared in the pericentromeric regions of the inactivated centromeres (Fig. 3*B* and *SI Appendix*, Fig. S4*A*). These neocentromeres are likely to be functional, considering that kinetochores were assembled successfully on all chromosomes (Fig. 3*A*). By crossing *mhf2Δcen1*$^{\text{inactive}}$ to wild-type (*mhf2*$^{+}$*cen1*$^{\text{active}}$), we recovered *mhf2*$^{+}$*cen1*$^{\text{inactive}}$ exhibiting wild-type growth among the progeny (Table 1 and *SI Appendix*, Fig. S4*B*). This suggests that the inactivated state of the original centromere (and presumably the accompanying neocentromere) appear mitotically stable (at least within tens of cell growth generations) in the absence of the genetic lesion that induced it. In *mhf2*$^{+}$*cen1*$^{\text{inactive}}$ and *mhf2*$^{+}$*cen2*$^{\text{inactive}}$, significant Cnp1 signals were detected in the pericentromeric regions of the inactivated centromeres by anti-Cnp1 ChIP-Seq (Fig. 3*B* and *SI Appendix*, Fig. S4*C*). Together with the low Cnp1 signal in *mhf2Δcen1*$^{\text{inactive}}$ and *mhf2Δcen2*$^{\text{inactive}}$, these results are consistent with the possibility that either Cnp1 incorporation at the neocentromeres is low in *mhf2Δ* or the positions of Cnp1 nucleosomes might be divergent among individual *mhf2Δ* cells within a population. Three individual Ndc80-GFP dots (representing 3 pairs of sister kinetochores) in early mitosis were visualized in *mhf2*$^{+}$*cen1*$^{\text{inactive}}$ after we introduced a conditional β-tubulin mutation (*nda3-KM311*) to allow the separation of the clustered centromeres at the restrictive temperature of *nda3-KM311*,

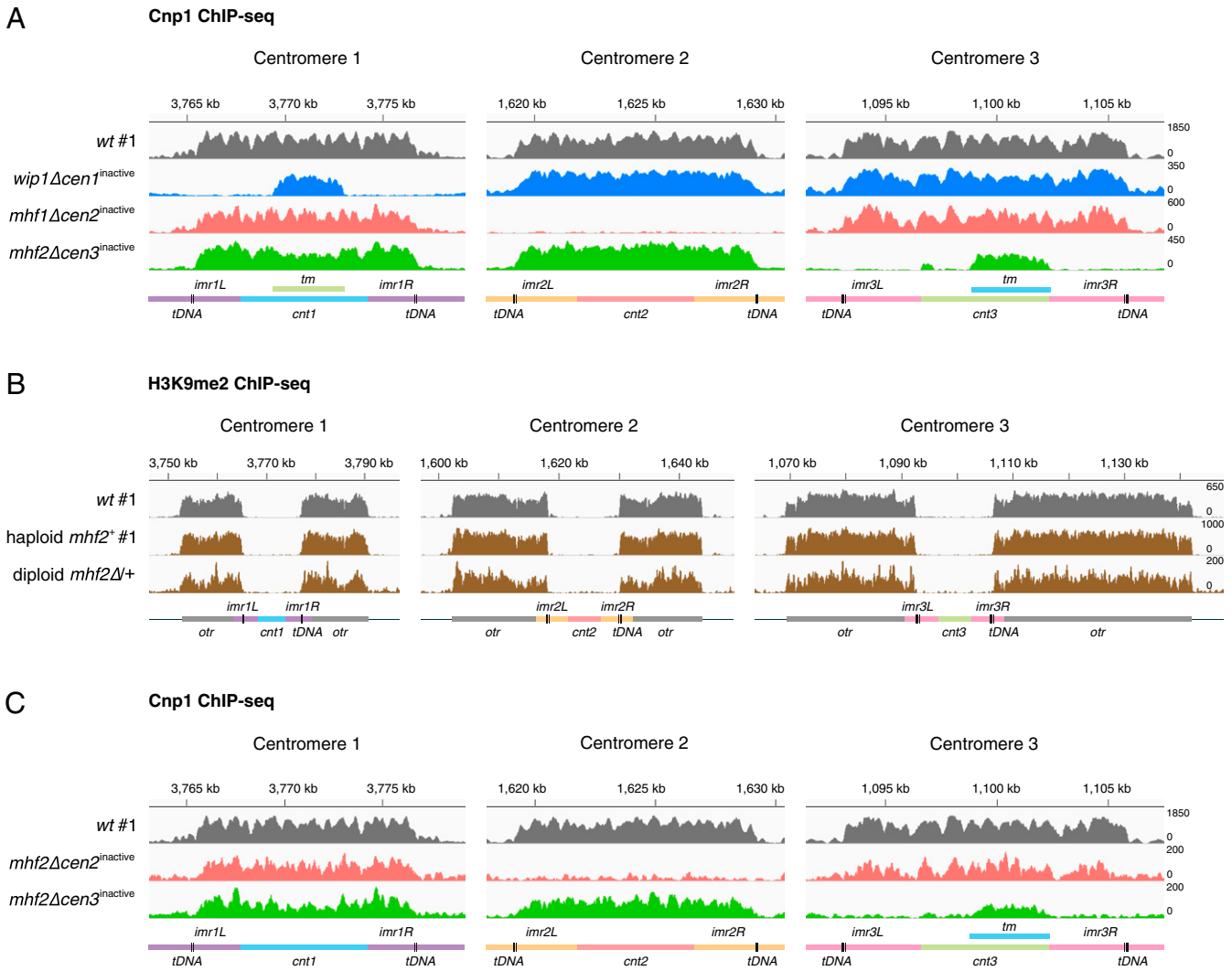

Fig. 2. Single depletion of CENP-T-W-S-X components induces centromere inactivation. (*A*) Cnp1 ChIP-seq reads mapped to centromeric regions of all 3 chromosomes in randomly chosen *wip1Δ*, *mhf1Δ*, and *mhf2Δ* strains (*cen1*^{inactive} blue, *cen2*^{inactive} pink, *cen3*^{inactive} green) compared to wild-type strain (*cen1/2/3*^{active} gray). (*B*) H3K9me2 ChIP-seq reads mapped to centromeric and pericentromeric regions of all 3 chromosomes in meiotic haploid progeny *mhf2*$^{+}$ and heterozygous deletion diploid *mhf2Δ/+* (brown) compared to wild-type cells (gray). (*C*) Cnp1 ChIP-seq reads mapped to centromeric regions of all 3 chromosomes in 2 *mhf2Δ* meiotic haploid progeny from the same tetrad (*cen2*^{inactive} pink, *cen3*^{inactive} green). #1, Biological replicate 1. Diagrams, *x* axis and *y* axis, same as in Fig. 1.

further confirming the formation of a neocentromere (*SI Appendix*, Fig. S4*D*). Together, these results demonstrate that pericentromeric heterochromatin is the preferable site for neocentromere formation.

Neocentromeres Occupy the Pericentromeric Repetitive Sequences Asymmetrically. Cnp1 spreading into the pericentromeric regions, as annotated bioinformatically, appears to be ubiquitous for all centromeres (see, for example, Fig. 5*A* and *SI Appendix*, Figs. S3*C*, S7*C*, and S8*C*). Furthermore, Cnp1 occupancy in the neocentromeres appears symmetrical on the pericentromeric repeats at both left and right sides of *cnt* (Fig. 3*B* and *SI Appendix*, Figs. S7*C* and S8 *B* and *C*; see also Fig. 5). However, due to high DNA sequence similarity between the pericentromeric repeats in all 3 centromeres (33), it is unclear whether such Cnp1 spreading and occupancy represents the physical footprint of Cnp1. To this end, by genetic crossing, we generated new strains carrying a neocentromere and a reporter gene *ura4* inserted into the right side of the repetitive regions of centromere 1 (*otr1R::ura4*) (see *SI Appendix*, *Materials and Methods* for details of genetic crosses). In strains carrying *cen2*^{inactive}, Cnp1 signals were detected on *otr1R::ura4* (Fig. 4 and *SI Appendix*, Fig. S5*B*), indicating Cnp1 occupancy at the *otr* repeats is not limited to the repositioned centromere, but rather is ubiquitous for all 3 centromeres. It is consistent with the observation that Cnp1 spreads onto all of the *imr* regions unique to each centromere. On the other hand, in 7 independent strains carrying *cen1*^{inactive}, cells showed no significant Cnp1 incorporation into *ura4* (Fig. 4 and *SI Appendix*, Fig. S5*A*). This excludes the possibility that Cnp1 occupancy on the repositioned centromere is symmetrical. Supporting this notion, in different strains exhibiting centromeric Cnp1 spreading, significant Cnp1 signals were detected on *ura4* in some strains but not in others (Fig. 4 and *SI Appendix*, Fig. S5). Consistently, we also found that the levels of heterochromatin (H3K9me2) and Cnp1 occupancy are inversely correlated on the *ura4* cassette (*SI Appendix*, Fig. S5*B*).

Heterochromatin occupies the site of the inactivated centromere, and neocentromeres are formed at the pericentromeric regions that were originally occupied by heterochromatin. These findings prompted us to further investigate whether heterochromatin plays a

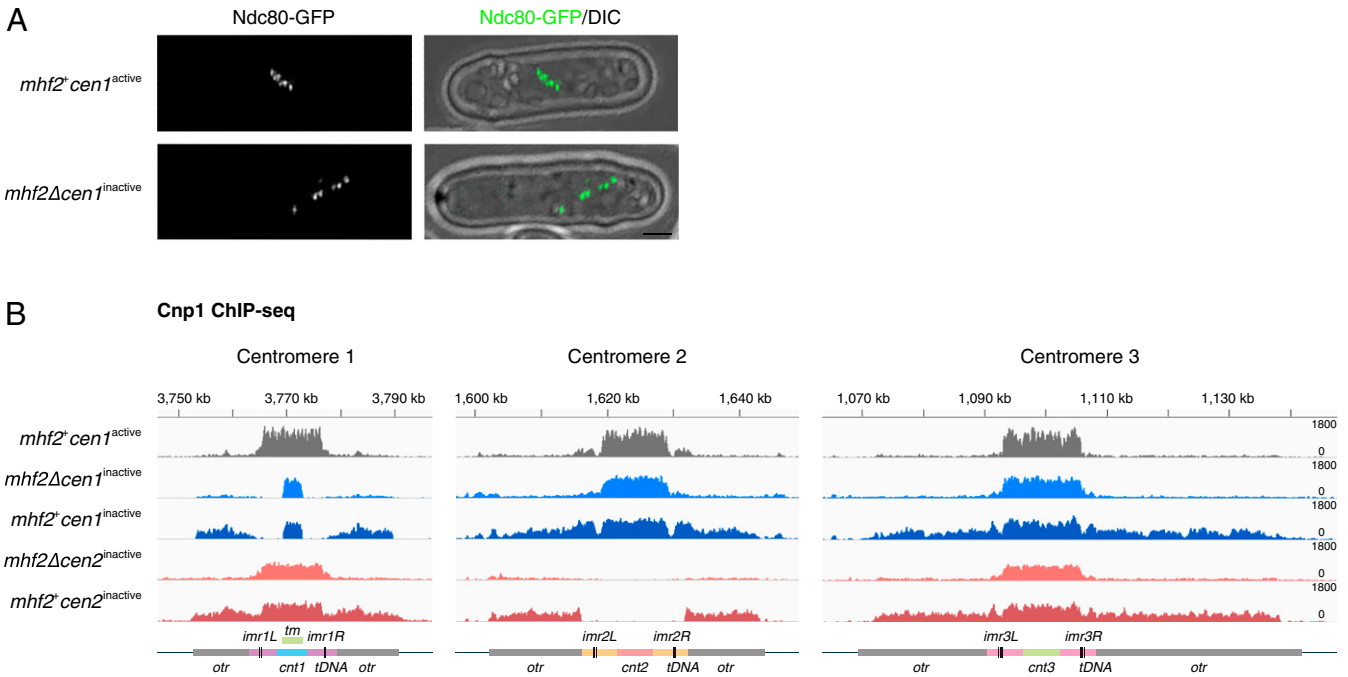

Fig. 3. Neocentromeres are formed preferentially in the pericentromeric regions. (*A*) Six dots of outer kinetochore Ndc80-GFP observed in *mhf2*$^{+}$*cen1*^{active} (*Upper*) and *mhf2Δcen1*^{inactive} (*Lower*) M phase cells treated with the thiabendazole (TBZ, 20 μg/mL). (Scale bar, 2 μm.) (*B*) Cnp1 ChIP-seq reads mapped to centromeric and pericentromeric regions of all 3 chromosomes in *mhf2Δcen1*^{inactive} (blue) and *mhf2*$^{+}$*cen1*^{inactive} (dark blue); *mhf2Δ cen2*^{inactive} (pink) and *mhf2*$^{+}$*cen2*^{inactive} (dark pink) compared to wild-type cells (gray). Diagrams, *x* axis and *y* axis, same as in Fig. 1.

role in centromere inactivation and neocentromere maintenance. To this end, we explored the possible impact of deletion of *clr4*, which encodes the only heterochromatin modification enzyme (H3K9 methyltransferase) for heterochromatin assembly in *S. pombe* (26). We deleted *clr4* in *mhf2Δcen2*^{inactive} (*SI Appendix*, Fig. S6*B*) or *mhf2*$^{+}$*cen1*^{inactive} haploid cells (*SI Appendix*, Fig. S6*C*) by DNA transformation and found that the inactivated centromeres and the neocentromeres were maintained. Together, these results suggest that mitotic maintenance of neocentromere does not require heterochromatin.

The Endogenous Centromere Tends to Be Converted Unilaterally to the Neocentromere in a Genetic Crossing Between Wild-Type and *mhf2Δ*. In genetic crosses between strains with mismatched centromeres (one carrying a neocentromere and the other an original centromere), a few asci produced 4 viable progeny, allowing reliable analysis of the inheritance of genetic lesions and epigenetic features (Table 1 and *SI Appendix*, Table S3). As expected, *mhf2Δ* conformed to Mendelian inheritance. Similarly, in *mhf2*$^{+}$*cen1*^{inactive} × *mhf2*$^{+}$*cen1*^{active}, *cen1*^{inactive} and the associated neocentromere also conformed to Mendelian inheritance, suggesting that they are meiotically stable (Fig. 5*A* and *SI Appendix*, Fig. S7). Furthermore, the progeny without *cen1*^{inactive} exhibited the spreading of centromeric Cnp1 into the pericentromeric regions in all centromeres, indicating a broad impact on centromeric chromatin due to *cen1*^{inactive} through meiosis (Fig. 5*A* and *SI Appendix*, Fig. S7*C*). Cnp1 spreading in all original centromeres was also found in the wild-type meiotic progeny of *wip1Δ*/+, *mhf1Δ*/+, and *mhf2Δ*/+ (*SI Appendix*, Fig. S3*C*). This broad alteration in centromeres might underscore the poor spore viability overall (*SI Appendix*, Table S1). In *mhf2Δcen1*^{inactive} × *mhf2*$^{+}$*cen1*^{active}, 2 independent asci (each with 4 viable progeny) were examined and, surprisingly, all of the progeny carry the *cen1*^{inactive} regardless of whether *mhf2*$^{+}$ or *mhf2Δ* was in the haploid genome (Fig. 5*B* and *SI Appendix*, Fig. S8*B*). In addition, in 9 other *mhf2*$^{+}$ progeny (derived from random spores) that were subjected to ChIP-seq analysis, 2 also exhibited *cen1*^{inactive}, whereas 7 displayed Cnp1 spreading in all 3 centromeres (*SI Appendix*,

Table 1. Incompatibility between neocentromeres and original centromeres causes a meiosis barrier

Cross	Spore viability, %	Dissected asci (*n*)	Asci with 4 viable spores, %	Asci with 1 or no viable spores, %	Meiosis barrier
mhf2^{+}*cen1*^{active} × *mhf2*$^{+}$*cen1*^{active}	93.1	130	80	1.54	×
mhf2^{+}*cen1*^{active} × *mhf2Δcen1*^{inactive}	36.5	254	5.9	53.1	√
mhf2^{+}*cen1*^{active} × *mhf2*$^{+}$*cen1*^{inactive}	25.2	272	4.04	69.5	√
mhf2^{+}*cen1*^{inactive} × *mhf2*$^{+}$*cen1*^{inactive} #1	89.8	108	68.5	1.9	×
mhf2^{+}*cen1*^{inactive} × *mhf2*$^{+}$*cen1*^{inactive} #2	31.4	106	9.4	62.3	√
mhf2^{+}*cen1*^{inactive} × *mhf2*$^{+}$*cen2*^{inactive}	19.8	377	0.8	81.2	√

Cells with mismatched (*mhf2*$^{+}$*cen1*^{active} × *mhf2Δcen1*^{inactive}, *mhf2*$^{+}$*cen1*^{active} × *mhf2*$^{+}$*cen1*^{inactive}, *mhf2*$^{+}$*cen1*^{inactive} × *mhf2*$^{+}$*cen1*^{inactive} #2, *mhf2*$^{+}$*cen1*^{inactive} × *mhf2*$^{+}$*cen2*^{inactive}) or matched (*mhf2*$^{+}$*cen1*^{active} × *mhf2*$^{+}$*cen1*^{active}, *mhf2*$^{+}$*cen1*^{inactive} × *mhf2*$^{+}$*cen1*^{inactive} #1) centromeres were crossed and subjected to tetrad dissection. Intact asci with 4 spores were dissected microscopically and scored for the number of viable spores. Spore viability is calculated as the ratio of the number of viable spores to the number of analyzed spores; >50% reduction in spore viability is defined as meiosis barrier and labeled as √, whereas no meiosis barrier is labeled as ×.

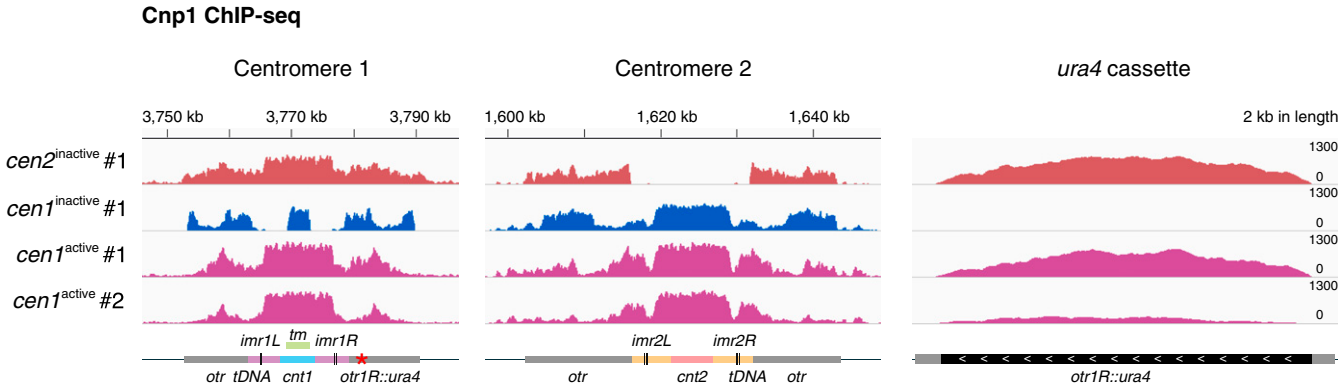

Fig. 4. Neocentromeres occupy the pericentromeric repetitive sequences asymmetrically. Cnp1 ChIP-seq reads mapped to centromeric and pericentromeric regions of all 3 chromosomes in *cen2*^{inactive} (dark pink), *cen1*^{inactive} (dark blue), and *cen1*^{active} with Cnp1 spreading (magenta). *ura4* cassette was inserted into the right side of the *otr1R* (*otr1R::ura4*) and labeled by a red asterisk. Chromosomes 1 and 2 and *ura4* cassette are shown. #1 and #2, Biological replicate 1 and 2. Diagrams, *x* axis and *y* axis, same as in Fig. 1.

Fig. S8*C*). Thus, *cen1*^{active} had a propensity to be converted into *cen1*^{inactive} in meiosis involving *mhf2Δ*, most likely using *cen1*^{inactive} on the homologous chromosome as the template. Although the mechanism remains unclear, this centromere conversion phenomenon highlights the pivotal role of *mhf2* in maintaining centromere identity in wild-type cells and a plausible way of propagating the neocentromere in a cell population of mixed karyotypes.

Incompatibility Between Neocentromeres and Endogenous Centromeres Causes a Meiosis Barrier. When crossed with wild-type (*cen1*/2/3^{active}), *mhf2Δcen1*^{inactive} showed high lethality of meiotic progeny. We also examined genetic crosses between wild-type (*cen1*/2/3^{active}) and *mhf2*$^{+}$*cen1*^{inactive}, and found that *mhf2*$^{+}$*cen1*^{inactive} causes a more severe reduction in progeny viability than *mhf2Δcen1*^{inactive} (Table 1). Strikingly, however, homozygotic meiosis (here, crossing between sister cells derived from the same ascus carrying the same neocentromere, *mhf2*$^{+}$*cen1*^{inactive} × *mhf2*$^{+}$*cen1*^{inactive} #1) exhibited near or at wild-type levels of spore viability (Table 1). These results demonstrate that *cen1*^{inactive} is competent for meiosis but a mismatch in centromeres between a pair of homologous chromosomes generates a reproductive barrier.

To test this further, we performed a series of genetic crosses among strains with different (*mhf2*$^{+}$*cen1*^{inactive} × *mhf2*$^{+}$*cen2*^{inactive}, *mhf2*$^{+}$*cen1*^{inactive} × *mhf2Δcen2*^{inactive} and *mhf2Δcen1*^{inactive} × *mhf2Δcen2*^{inactive}) or the same (*mhf2*$^{+}$*cen1*^{inactive} × *mhf2Δcen1*^{inactive}) centromeres and determined spore viability (Table 1 and *SI Appendix*, Tables S3 and S4). Together, the results demonstrate that a mismatch between a neocentromere and the original centromere on any 1 chromosome alone causes poor spore viability, and that the spore viability is further reduced as the number of mismatched centromeres increased. We also found crosses between certain strains carrying the *cen1*^{inactive} (each with a neocentromere somewhere in the pericentromeric regions of chromosome 1; i.e., *mhf2*$^{+}$*cen1*^{inactive} × *mhf2*$^{+}$*cen1*^{inactive} #2) showed significant loss of spore viability (Table 1). This is consistent with the notion that the locations of neocentromeres are asymmetric relative to the centromeric cores and may be different from each other in these 2 strains.

To obtain cytological evidence for the meiosis barrier caused by mismatched centromeres, we inserted a GFP tag at the *lys1* locus close to *cen1* using the *lacOs*/lacI-GFP system (designated as *cen1*-GFP hereafter) to microscopically track chromosome 1 segregation during meiosis. In this system, when chromosome 1 of both parental haploid cells are labeled with *cen1*-GFP, the 4-dot distribution pattern among the meiotic progeny indicates the segregation of sister and homologous chromosome 1 (Fig. 6*A*). When only 1 parental haploid cell carries the *cen1*-GFP, the 2-dot distribution pattern indicates the segregation of the tagged sister chromosome 1 (Fig. 6*B*). We identified and categorized the abnormal chromosome segregation patterns into different types. For example, type II and type III of 2-dot distribution suggest premature segregation of sister chromatids in meiosis I and missegregation of sister chromatids in meiosis II, respectively (Fig. 6*B*). As expected, we found severe sister and homologous chromosome segregation defects in both meiosis I and II in zygotic meiosis with mismatched centromere 1 (cross B in Fig. 6*A* and cross E in *SI Appendix*, Fig. S9*A*; cross 2 in Fig. 6*B* and cross 5 in *SI Appendix*, Fig. S9*B*). We also noticed that the meiotic defects were not confined to the mismatched centromeres; when *mhf2*$^{+}$*cen2*^{active} cells carrying the *cen1*-GFP were crossed to *mhf2Δcen2*^{inactive} cells with a mismatched *cen2*, chromosome 1 also exhibited segregation defects (cross 6 in *SI Appendix*, Fig. S9*B*), but not as severe as that in mismatched centromeres (cross 2 in Fig. 6*B* and cross 5 in *SI Appendix*, Fig. S9*B*). Overall, these results demonstrate that mismatched centromeres between homologous chromosome pairs cause hybrid infertility due to severe meiotic defects, and thus constitute a meiosis barrier between the 2 strains.

Homozygotic Repositioned Centromeres Frequently Undergo Meiotic Segregation Events in an Inverted Order. In homozygotic meiosis with the same neocentromere 1 or 2, 4 copies of chromosome 1 (visualized with *cen1*-GFP) were evenly segregated to the 4 spores in most asci (crosses C and D in Fig. 6*A*; crosses F and G in *SI Appendix*, Fig. S9*A*). Surprisingly, in homozygotic meiosis with the same neocentromere 1 but where only one was labeled with *cen1*-GFP, 73.5% of the zygotes at anaphase of meiosis I exhibited premature separation of sister *cen1*-GFP dots (cross 3 in Fig. 7*A*). Consistently, in 65 to 75% of the asci, 2 *cen1*-GFP dots no longer occupied sister-spore positions (cross 3 in Fig. 6*B*; crosses 7 and 8 in *SI Appendix*, Fig. S9*B*). Nonetheless, these crosses displayed wild-type levels of spore viability (Fig. 7*B* and *SI Appendix*, Fig. S9*C*), indicating eventual success in accurate meiotic chromosome segregation. This is in agreement with the results (Table 1) that spore viability of genetic crosses between cells carrying the same neocentromeres was comparable to the wild-type level (*SI Appendix*, Table S3). On the other hand, in a comparable genetic cross in which both strains carried *cen2*^{inactive} but only 1 parental haploid was labeled with *cen1*-GFP, the majority of the labeled sister chromosome 1 segregation occurred in meiosis II and strictly followed the canonical order of meiosis I and meiosis II (cross 4 in Figs. 6*B* and 7*A*).

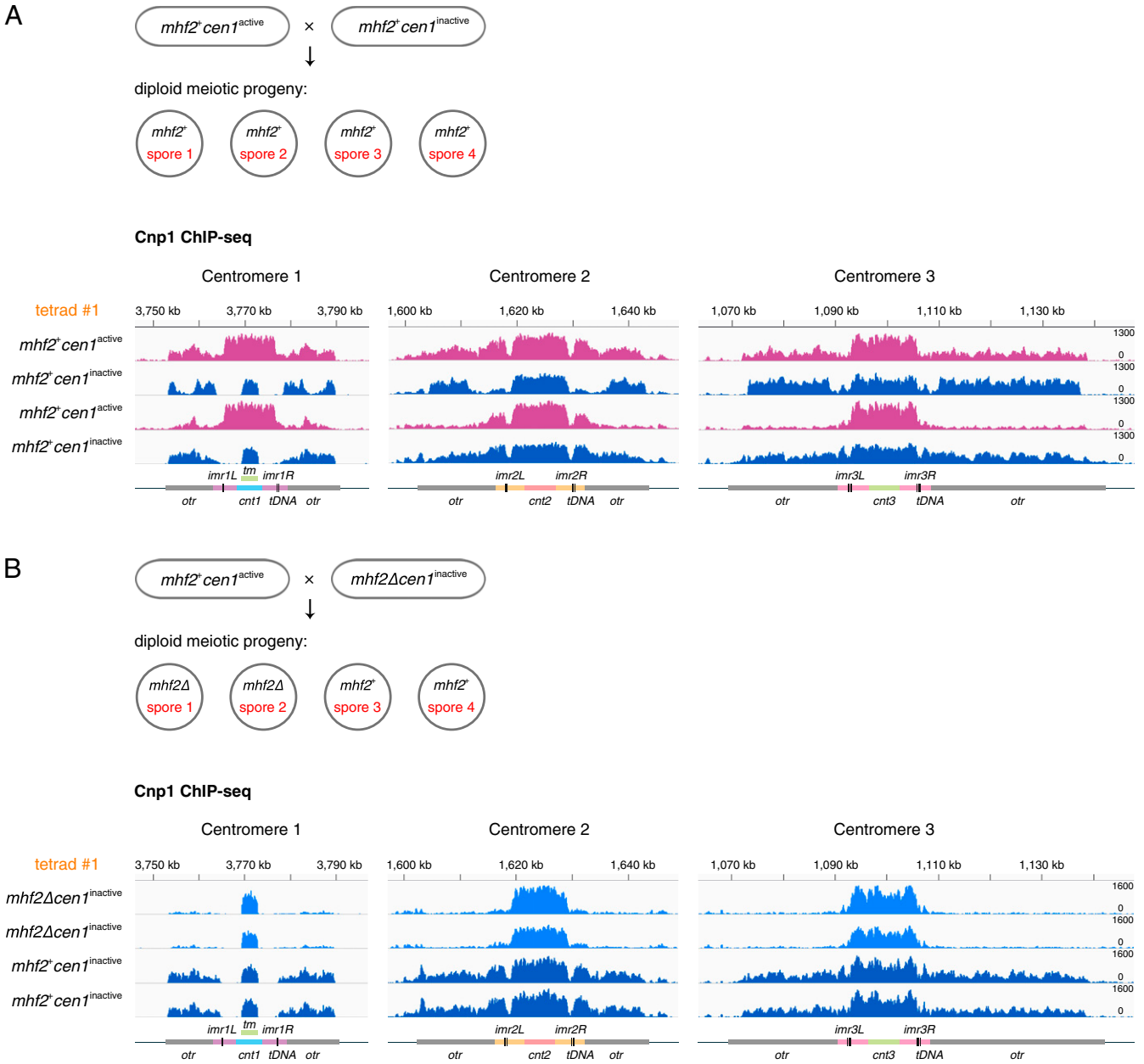

Fig. 5. The endogenous centromere in *mhf2*$^+$ cells tends to be converted to an inactivated centromere by *mhf2Δ* through meiosis. (*A*) Schematic illustrates the meiotic progeny of *mhf2*$^+$*cen1*^{active} × *mhf2*$^+$*cen1*^{inactive} in asci with 4 spores. Cnp1 ChIP-seq reads mapped to centromeric and pericentromeric regions of all 3 chromosomes in 4 viable meiotic progeny from the same ascus (tetrad #1) of *mhf2*$^+$*cen1*^{active} × *mhf2*$^+$*cen1*^{inactive}. *mhf2*$^+$*cen1*^{inactive} (dark blue) conformed to Mendelian inheritance (2: 2 segregation pattern). *mhf2*$^+$*cen1*^{active} (magenta) exhibits the spreading of Cnp1 into the pericentromeric regions. See *SI Appendix*, Fig. S7*B* for accompanying H3K9me2 ChIP-seq data. (*B*) Schematic illustrates the meiotic progeny of *mhf2*$^+$*cen1*^{active} × *mhf2Δcen1*^{inactive} in asci with 4 spores. Same procedure as in *A* for analyzing *mhf2*$^+$*cen1*^{active} × *mhf2Δcen1*^{inactive}. *mhf2Δ* conformed to Mendelian inheritance (2: 2 segregation pattern). *cen1*^{inactive} was detected in *mhf2*$^+$ (dark blue) and *mhf2Δ* (blue). See *SI Appendix*, Fig. S8*B* for accompanying H3K9me2 ChIP-seq data. Diagrams, *x* axis and *y* axis, same as in Fig. 1.

To rule out the possibility that the observed early segregation of sister chromosome 1 may be due to highly frequent crossing-over between *cen1* and the *cen1*-GFP tag (~10 kb to the left edge of *cen1*), we tested the genetic linkage between *otr1R::ura4* and *cen1*-GFP markers in these genetic crosses (Fig. 7*C*). We found 1.42% (n = 352) crossing over between these 2 loci in homozygotic repositioned centromere 1, comparable to that of the homozygotic original centromere 1 (1.47%, n = 272), ruling out the possibility of a recombination hotspot between the repositioned centromere 1 and the *cen1*-GFP tag.

Collectively, these results demonstrate that chromosomes carrying neocentromeres frequently invert the order of meiotic chromosome segregation events (i.e., sister chromatids segregate first and homologous chromosomes separate second) and that inverted meiosis is restricted to neocentromeres. Furthermore, the successful completion of meiosis and high progeny viability suggest that canonical and inverted meiosis on different chromosomes occur concomitantly in the same cell and thus, must be mechanistically compatible with each other.

Discussion

Centromere Repositioning Induced by the Inner Kinetochore Impairment. Our study shows that genetic abrogation of the inner kinetochore (such as subunits of the CENP-T-W-S-X complex) in fission yeast

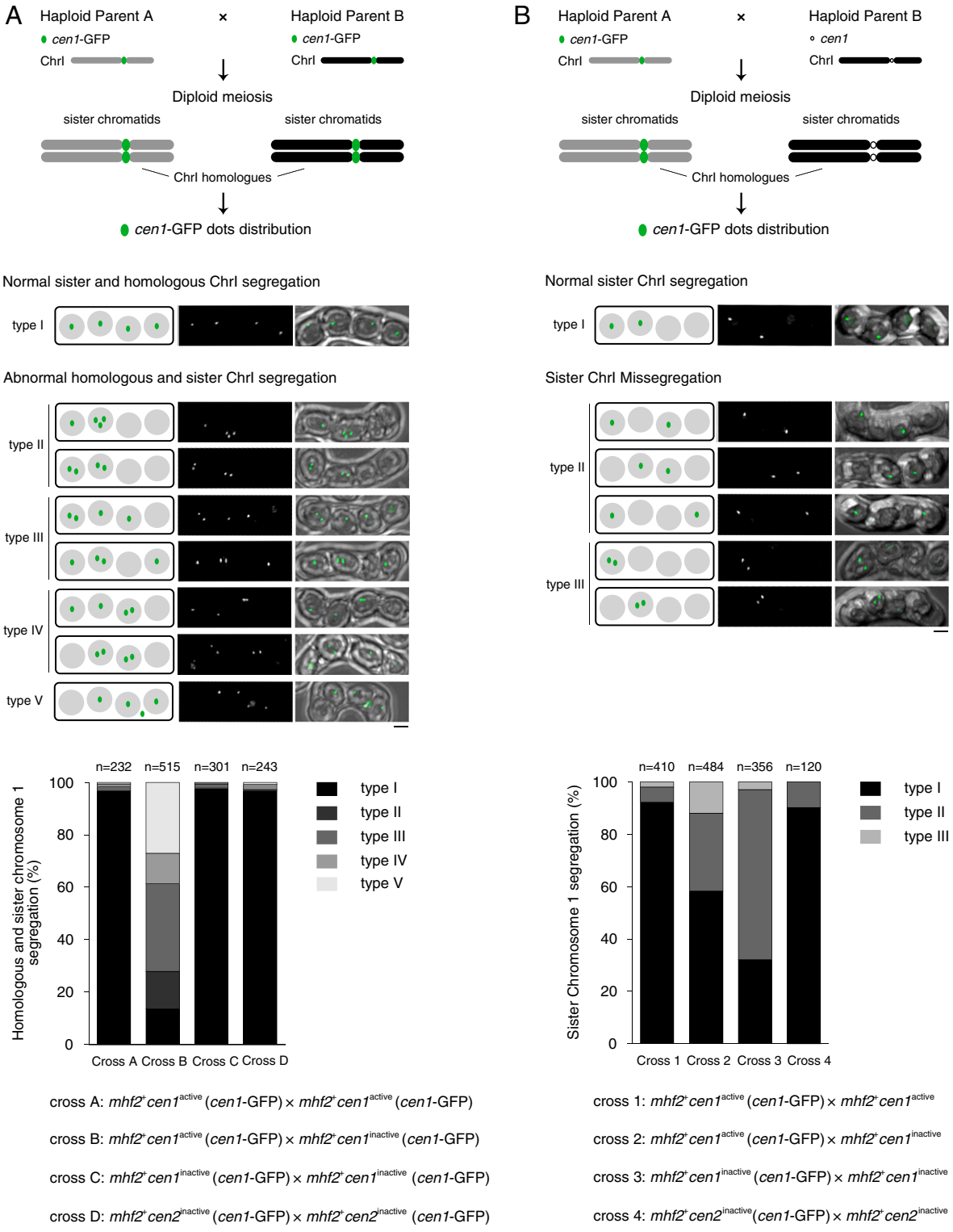

Fig. 6. Homozygotic meiosis with matched neocentromeres exhibits premature segregation of sister chromatids. (*A*) Schematic illustrates the meiotic segregation of chromosome 1 (ChrI) in the genetic cross between haploid parent A (gray) and haploid parent B (black), both cells carrying the chromosome 1 marker—*lys1* locus decorated with GFP (*lys1::lacOs/lacI-GFP*)—designated as *cen1*-GFP (green dot). The distributions of *cen1*-GFP are categorized into 5 types (type I to type V). (Scale bar, 2 μm.) Cross A-B, $mhf2^{+}cen1^{active}$ cells crossed to $mhf2^{+}cen1^{active}$ and $mhf2^{+}cen1^{inactive}$ cells, respectively; cross C, $mhf2^{+}cen1^{inactive}$ cells crossed to $mhf2^{+}cen1^{inactive}$ cells; cross D, $mhf2^{+}cen2^{inactive}$ cells crossed to $mhf2^{+}cen2^{inactive}$ cells. The *cen1*-GFP dots were scored in 4-spored asci to trace the meiotic segregation of homologous chromosome 1 and sister chromosome 1. *n*, the total 4-spored asci analyzed. (*B*) Schematic illustrates the meiotic segregation of chromosome 1 (ChrI) in the genetic cross between haploid parent A (gray) carrying the *cen1*-GFP and haploid parent B (black). Black circle, centromere 1 without GFP labeling (*cen1*). The distributions of *cen1*-GFP are categorized into 3 types (type I to type III). (Scale bar, 2 μm.) Crosses 1 and 2, $mhf2^{+}cen1^{active}$ cells crossed to $mhf2^{+}cen1^{active}$ and $mhf2^{+}cen1^{inactive}$ cells, respectively; cross 3, $mhf2^{+}cen1^{inactive}$ cells crossed to $mhf2^{+}cen1^{inactive}$ cells; cross 4, $mhf2^{+}cen2^{inactive}$ cells crossed to $mhf2^{+}cen2^{inactive}$ cells. The *cen1*-GFP dots were scored in 4-spored asci to trace the meiotic segregation of sister chromosome 1. *n*, the total 4-spored asci analyzed.

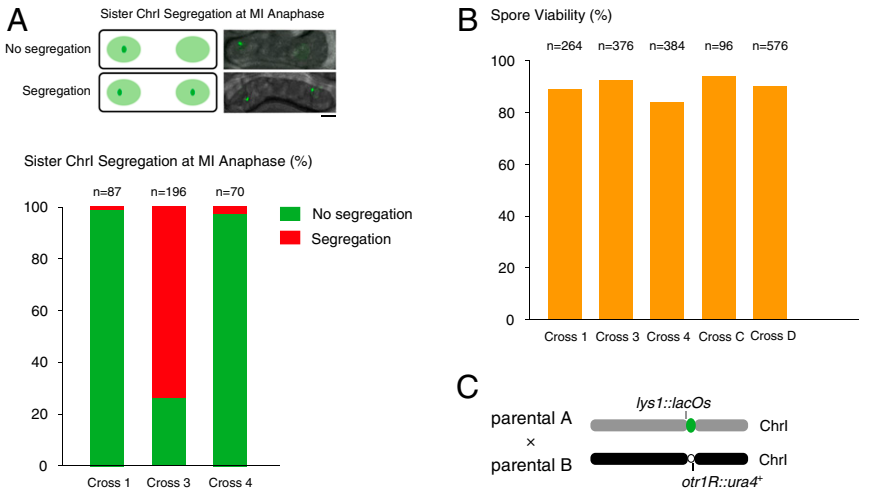

Fig. 7. Homozygotic repositioned centromeres undergo meiotic segregation events in an inverted order and exhibit wild-type level spore viability. (*A*) Schematic illustrates the segregation pattern of sister chromosome 1 at anaphase during meiosis I (MI anaphase). (Scale bar, 2 μm.) The graph plots the percentage of MI anaphase cells displaying cosegregation (green) or presegregation (red) of sister chromosome 1 in homozygotic meiosis. *n*, The total counted MI anaphase cells. (*B*) Intact asci with 4 spores from the above genetic crosses were dissected microscopically and scored for the number of viable spores. Spore viability was calculated as the ratio of the number of viable spores to the number of analyzed spores. *n*, The total spores analyzed. (*C*) Schematic illustrates the assay calculating the crossover rates of regions nearby the centromere between parental A (*lys1::lacOs/lacI-GFP*) and parental B (*otr1R::ura4*).

readily initiates centromere repositioning but is dispensable for the mitotic maintenance of neocentromeres (Fig. 8*A*). Together, these results reveal a fundamental and evolutionarily conserved role of the kinetochore in maintaining centromere epigenetic identity, and suggest that inducing neocentromere formation without incurring centromeric DNA changes or chromosomal rearrangements could be rapid and efficient in contrast to prior speculation that centromere repositioning might be a gradual, long evolutionary process (1, 34, 35).

A recent study reported that in cultured chicken DT40 cells, knocking out nonessential constitutive kinetochore components, including CENP-S, enhances centromere drift within a defined small region on the chromosome upon prolonged cell proliferation, consistent with the role of the inner kinetochore CENP-T-W-S-X complex in stabilizing centromeres (36). However, in chicken cells, centromere drifting reflects enhanced dynamicity of centromeres between mitotic cell generations, whereas in fission yeast cells, once the centromere moves to a new location, it is stable mitotically and meiotically. Thus, in these 2 systems, CENP-T-W-S-X depletion may disrupt different aspects of centromere epigenetic stability.

In addition to the perturbation of inner kinetochore components, meiosis seems to actively facilitate the processes of centromere repositioning as its efficiency in the *mhf2Δ* progeny of heterozygous diploid (*mhf2Δ*/+) meiosis or genetic crossings is 100% (15 independent strains tested), in contrast to that induced by the removal of whole *cen1* DNA (about 0.06%) (32). We speculate that an unidentified step of meiosis may trigger centromeric chromatin reprogramming during neocentromere formation. We were unable to delete *mhf2* directly in haploid cells and thus cannot determine whether it is possible to induce centromere repositioning in mitotic cells. However, its frequent occurrence through meiosis suggests an important role of meiotic processes in inducing the repositioned centromere. We also find that *mhf2Δ* tends to convert the original centromere in $mhf2^+$ into the inactivated state, which should accelerate the propagation of neocentromeres in the population through meiosis.

Together, these results suggest that centromere repositioning should be a relatively prevalent phenomenon, yet few neocentromeres have been detected so far. One possible explanation is the experimental limitations on their detection: The karyotype of most organisms has traditionally been determined by cytogenetic analysis usually in only a few individuals except in clinical human samples; and small changes in centromere position may evade detection by classic cytogenetic techniques because of low resolution. In addition, neocentromeres and the mutations that induce their formation may cause detrimental effects on cell fitness resulting in their underrepresentation or elimination.

The Properties of Neocentromeres. Neocentromeres have a propensity to locate on either side of the original inactivated centromere. This is in contrast to the scenario in which a neocentromere was formed near the subtelomeric heterochromatin regions upon complete removal of *cen* DNA, including the pericentromeric repeats in fission yeast (32), suggesting that pericentromeric regions are preferable to subtelomeric regions for neocentromere formation. In wild-type cells, a trace amount of Cnp1 was captured on the pericentromeric regions compared with the centromeric core regions (10, 37). Hence, it is likely that residual Cnp1 seeds the formation of neocentromeres and explains the preference for pericentromeric regions. Consistently, neocentromere formation at pericentromeric regions has been found in other organisms with complete removal of *cen* DNA (38–40).

Our data demonstrate that Cnp1 and H3K9me2 are mutually exclusive (*SI Appendix*, Fig. S5*B*), and that heterochromatin is not required for mitotic maintenance of the repositioned centromeres. Heterochromatin spreading is likely consequential to centromere perturbation and inactivation, although the possibility that heterochromatin to some extent contributes to neocentromere formation cannot be completely ruled out. It is also possible that other molecular features or processes in the pericentromeric region such as noncoding RNA transcription or small interfering RNA processing may favor neocentromere formation. Recently, 3D genomic architecture analysis suggested that neocentromeres physically interact with distant heterochromatin domains (41). Combining these observations, we propose that molecular processes or properties other than histone H3K9 methylation of the heterochromatin domain per se might play a pivotal role in neocentromere formation.

A Mechanism for Reproductive Barrier: Heterozygotic Repositioned Centromeres. One important functional consequence of centromere repositioning in fission yeast is that mismatching between

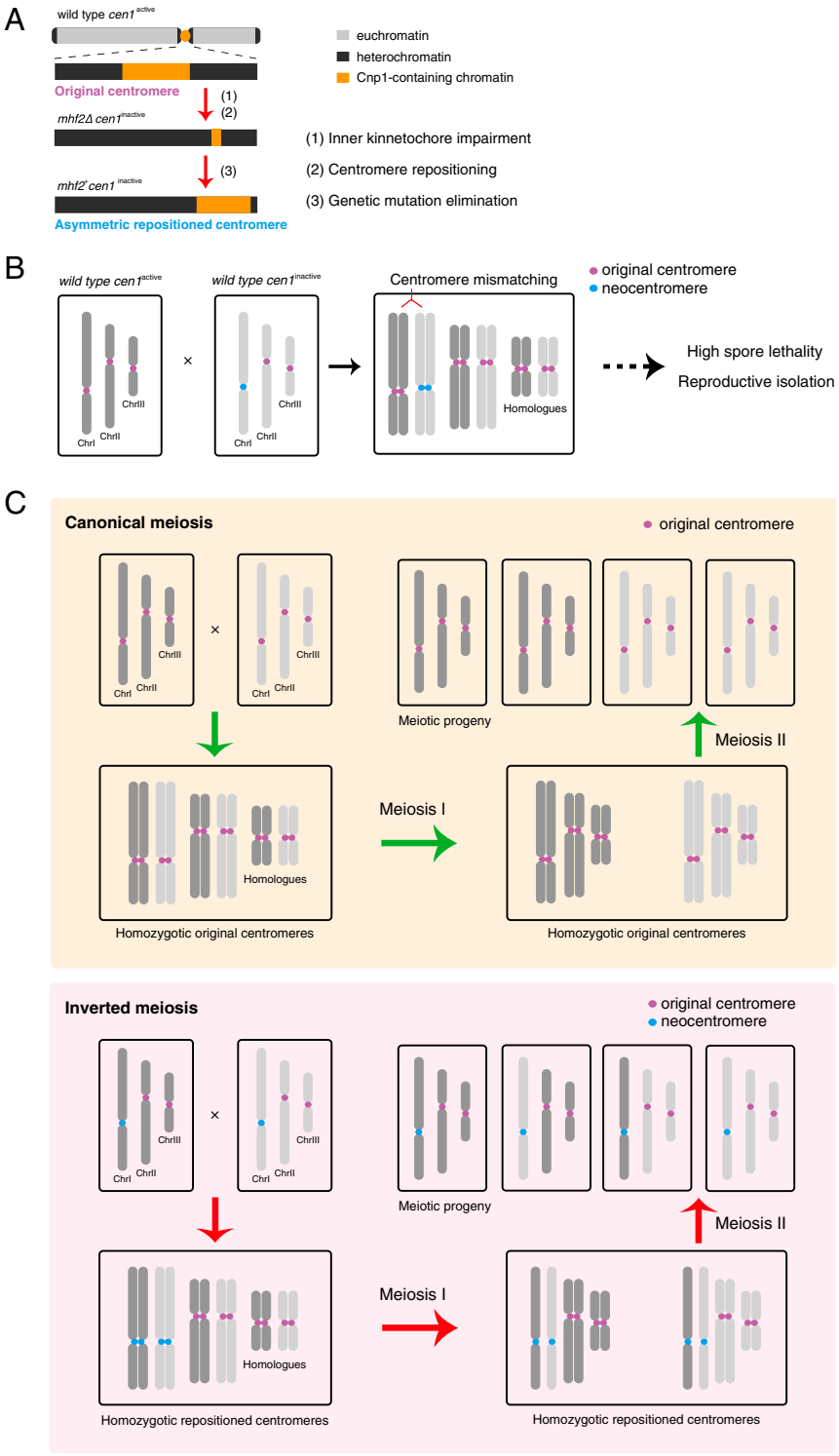

Fig. 8. Model diagram of centromere repositioning. (*A*) Centromere inactivation is induced by impairment of the inner kinetochore, with subsequent asymmetric neocentromere formation preferentially at the pericentromeric regions. (*B*) Centromere mismatching between an original centromere (*cen1*^{active}) and a neocentromere (*cen1*^{inactive}) generates a reproductive barrier by causing severe spore lethality. (*C*) Canonical meiosis with homozygotic original centromeres (*Upper*) and inverted meiosis with homozygotic neocentromeres (*Lower*) both generate four viable meiotic progeny. In canonical meiosis, sister chromatids are cosegregated in first meiotic division (meiosis I) and are separated in the second meiotic division (meiosis II). In inverted meiosis, sister chromatids are disassociated from each other during meiosis I and the homologs are segregated during meiosis II. For simplicity, other features of meiosis including crossover, recombination between homologs and random segregation of homologs are omitted in this diagram.

the original centromere and the neocentromere causes a reduction in the efficiency of meiosis (Fig. 8*B*). We notice that severe meiotic chromosome segregation defects are not limited to the mismatched centromeres, but are also detected (albeit to a lesser extent) in other centromere pairs, suggesting that the impact on meiosis is global (Fig. 6*B* and *SI Appendix*, Fig. S9*B*).

The specific causes of these meiotic defects remains unclear and may be due to disruption of processes related to homologous centromeres, such as centromere pairing in early meiosis, or recombination repression at centromeres (42). We speculate that the potential conflict in executing different modes of meiosis (i.e., the canonical and the inverted meiosis) (Fig. 8*C*) for the same pair of homologous chromosomes could be a major cause for this reproductive barrier.

To our knowledge, no previous studies have described the specific functional impact or potential meiotic complications caused solely by centromere repositioning. On the other hand, ample evidence of ENCs strongly implies that neocentromeres may play an important role in speciation (5). However, direct experimental evidence is unavailable because established cases of heterogeneity in centromere positioning are lacking (a notable exception is orangutans, whose centromere of chromosome 12 exhibits alternative positions in about 20% of the population, but unfortunately, are not readily amendable to experimentation) (43, 44). By showing that heterozygous but not homozygous meiosis is defective, our results provide the experimental support that neocentromeres seen as ENCs represent an initiation step for genetic divergence during speciation (44–46). As a mechanism of establishing a meiosis barrier (Fig. 8*B*), the efficiency of mismatched centromeres is comparable to that of other known mechanisms in fission yeast including chromosomal rearrangements (47) and spore killer genes (48, 49).

Inverted Meiosis in Monocentric Organisms. Unexpectedly, centromere repositioning frequently causes inversion of the order of 2 nuclear divisions in a homozygotic meiosis (Fig. 8*C*). Inverted meiosis has been observed in multiple species, all of which have holocentromeres. The canonical meiosis program requires sequential resolution of cohesion on chromosome arms and centromeric cohesion, which is incompatible with holocentromeres. Organisms with holocentromeres bypass this obstacle using various strategies, one of which being inverted meiosis (18–21). However, a recent study in human female germline, by tracking the distribution of homolog-specific genetic markers (SNPs) in mature oocytes and polar bodies during meiosis in vitro using single-cell whole-genome sequencing, has found that reversed segregation/inverted meiosis can also occur in a monocentric organism (22). Here, we present cytological evidence in fission yeast, a traditional model organism for studying canonical meiosis, that relocating a monocentromere to a nearby position frequently induces inverted meiosis, lending strong support to the notion that inverted meiosis might not be an exception but rather, may occur commonly in many organisms, and can be revealed by appropriate experimental approaches (for example, the human female meiosis study) or under suitable conditions, such as centromere repositioning in fission yeast.

Inversion in the order of meiotic chromosome segregation events imposes major mechanistic challenges. To segregate sister chromatids equally in meiosis I, sister kinetochores must now establish bipolar (biorientation) instead of monopolar attachment to the spindle (co-orientation) in canonical meiosis; and cohesion must be resolved completely along the whole chromosome, including the centromeres. We speculate that centromere repositioning somehow alters the local chromatin organization, rendering sufficient flexibility to sister kinetochore geometry that is compatible with both the biorientation required for sister chromatids separation and the co-orientation necessary for sister chromatids cosegregation. On the other hand, to ensure homologous chromosome disjunction in meiosis II in inverted meiosis, linkage between the homologs should be in place prior to their segregation. Further studies are needed to validate the existence and the molecular nature of such linkage, and to explore whether the established, recombination-dependent mechanisms or new, recombination-independent mechanisms are employed.

Materials and Methods

Details of the materials and methods, including strain construction, ChIP-seq and data analysis, microscopy, spore viability, and data availability are presented in *SI Appendix, Materials and Methods*.

ACKNOWLEDGMENTS. We thank Shiv Grewal, Lilin Du, and Robin Allshire for providing strains and reagents; and Shelley Sazer, Zheng Zhou, Xing Guo, Jun Ma, and Mariano Rocchi for the valuable discussions. This work was supported by National 973 Plan for Basic Research Grant 2015CB910602 (to X.H.) and National Natural Science Foundation of China Grant 31628012 (to X.H.).

1. T. Fukagawa, W. C. Earnshaw, The centromere: Chromatin foundation for the kinetochore machinery. *Dev. Cell* **30**, 496–508 (2014).
2. D. W. Cleveland, Y. Mao, K. F. Sullivan, Centromeres and kinetochores: From epigenetics to mitotic checkpoint signaling. *Cell* **112**, 407–421 (2003).
3. F. G. Westhorpe, A. F. Straight, The centromere: Epigenetic control of chromosome segregation during mitosis. *Cold Spring Harb. Perspect. Biol.* **7**, a015818 (2014).
4. D. J. Amor, K. H. Choo, Neocentromeres: Role in human disease, evolution, and centromere study. *Am. J. Hum. Genet.* **71**, 695–714 (2002).
5. O. J. Marshall, A. C. Chueh, L. H. Wong, K. H. Choo, Neocentromeres: New insights into centromere structure, disease development, and karyotype evolution. *Am. J. Hum. Genet.* **82**, 261–282 (2008).
6. M. Rocchi, N. Archidiacono, W. Schempp, O. Capozzi, R. Stanyon, Centromere repositioning in mammals. *Heredity* **108**, 59–67 (2012).
7. O. Capozzi *et al.*, Evolutionary and clinical neocentromeres: Two faces of the same coin? *Chromosoma* **117**, 339–344 (2008).
8. I. M. Cheeseman, The kinetochore. *Cold Spring Harb. Perspect. Biol.* **6**, a015826 (2014).
9. H. D. Folco *et al.*, The CENP-A N-tail confers epigenetic stability to centromeres via the CENP-T branch of the CCAN in fission yeast. *Curr. Biol.* **25**, 348–356 (2015).
10. M. Lu, X. He, Ccp1 modulates epigenetic stability at centromeres and affects heterochromatin distribution in *Schizosaccharomyces pombe*. *J. Biol. Chem.* **293**, 12068–12080 (2018).
11. K. Takahashi, E. S. Chen, M. Yanagida, Requirement of Mis6 centromere connector for localizing a CENP-A-like protein in fission yeast. *Science* **288**, 2215–2219 (2000).
12. K. Tanaka, H. L. Chang, A. Kagami, Y. Watanabe, CENP-C functions as a scaffold for effectors with essential kinetochore functions in mitosis and meiosis. *Dev. Cell* **17**, 334–343 (2009).
13. S. J. Falk *et al.*, Chromosomes. CENP-C reshapes and stabilizes CENP-A nucleosomes at the centromere. *Science* **348**, 699–703 (2015).
14. L. Y. Guo *et al.*, Centromeres are maintained by fastening CENP-A to DNA and directing an arginine anchor-dependent nucleosome transition. *Nat. Commun.* **8**, 15775 (2017).
15. H. Sato, F. Masuda, Y. Takayama, K. Takahashi, S. Saitoh, Epigenetic inactivation and subsequent heterochromatinization of a centromere stabilize dicentric chromosomes. *Curr. Biol.* **22**, 658–667 (2012).
16. D. Zickler, N. Kleckner, Recombination, pairing, and synapsis of homologs during meiosis. *Cold Spring Harb. Perspect. Biol.* **7**, a016626 (2015).
17. Y. Watanabe, Geometry and force behind kinetochore orientation: Lessons from meiosis. *Nat. Rev. Mol. Cell Biol.* **13**, 370–382 (2012).
18. M. Schvarzstein, S. M. Wignall, A. M. Villeneuve, Coordinating cohesion, co-orientation, and congression during meiosis: Lessons from holocentric chromosomes. *Genes Dev.* **24**, 219–228 (2010).
19. G. Cabral, A. Marques, V. Schubert, A. Pedrosa-Harand, P. Schlögelhofer, Chiasmatic and achiasmatic inverted meiosis of plants with holocentric chromosomes. *Nat. Commun.* **5**, 5070 (2014).
20. S. Heckmann *et al.*, Alternative meiotic chromatid segregation in the holocentric plant Luzula elegans. *Nat. Commun.* **5**, 4979 (2014).
21. V. A. Lukhtanov *et al.*, Versatility of multivalent orientation, inverted meiosis, and rescued fitness in holocentric chromosomal hybrids. *Proc. Natl. Acad. Sci. U.S.A.* **115**, E9610–E9619 (2018).
22. C. S. Ottolini *et al.*, Genome-wide maps of recombination and chromosome segregation in human oocytes and embryos show selection for maternal recombination rates. *Nat. Genet.* **47**, 727–735 (2015).
23. R. C. Allshire, K. Ekwall, Epigenetic regulation of chromatin states in Schizosaccharomyces pombe. *Cold Spring Harb. Perspect. Biol.* **7**, a018770 (2015).
24. S. Murakami, T. Matsumoto, O. Niwa, M. Yanagida, Structure of the fission yeast centromere cen3: Direct analysis of the reiterated inverted region. *Chromosoma* **101**, 214–221 (1991).
25. N. C. Steiner, K. M. Hahnenberger, L. Clarke, Centromeres of the fission yeast Schizosaccharomyces pombe are highly variable genetic loci. *Mol. Cell. Biol.* **13**, 4578–4587 (1993).
26. J. Nakayama, J. C. Rice, B. D. Strahl, C. D. Allis, S. I. S. Grewal, Role of histone H3 lysine 9 methylation in epigenetic control of heterochromatin assembly. *Science* **292**, 110–113 (2001).
27. K. C. Scott, S. L. Merrett, H. F. Willard, A heterochromatin barrier partitions the fission yeast centromere into discrete chromatin domains. *Curr. Biol.* **16**, 119–129 (2006).

28. T. Hayashi *et al*., Mis16 and Mis18 are required for CENP-A loading and histone deacetylation at centromeres. *Cell* **118**, 715–729 (2004).
29. E. S. Chen, S. Saitoh, M. Yanagida, K. Takahashi, A cell cycle-regulated GATA factor promotes centromeric localization of CENP-A in fission yeast. *Mol. Cell* **11**, 175–187 (2003).
30. E. M. Dunleavy *et al*., A NASP (N1/N2)-related protein, Sim3, binds CENP-A and is required for its deposition at fission yeast centromeres. *Mol. Cell* **28**, 1029–1044 (2007).
31. T. Nishino *et al*., CENP-T-W-S-X forms a unique centromeric chromatin structure with a histone-like fold. *Cell* **148**, 487–501 (2012).
32. K. Ishii *et al*., Heterochromatin integrity affects chromosome reorganization after centromere dysfunction. *Science* **321**, 1088–1091 (2008).
33. Y. Nakaseko, Y. Adachi, S. Funahashi, O. Niwa, M. Yanagida, Chromosome walking shows a highly homologous repetitive sequence present in all the centromere regions of fission yeast. *EMBO J.* **5**, 1011–1021 (1986).
34. I. Schubert, M. A. Lysak, Interpretation of karyotype evolution should consider chromosome structural constraints. *Trends Genet.* **27**, 207–216 (2011).
35. I. Schubert, What is behind "centromere repositioning"? *Chromosoma* **127**, 229–234 (2018).
36. T. Hori *et al*., Constitutive centromere-associated network controls centromere drift in vertebrate cells. *J. Cell Biol.* **216**, 101–113 (2017).
37. E. S. Choi, Y. Cheon, K. Kang, D. Lee, The Ino80 complex mediates epigenetic centromere propagation via active removal of histone H3. *Nat. Commun.* **8**, 529 (2017).
38. W. H. Shang *et al*., Chromosome engineering allows the efficient isolation of vertebrate neocentromeres. *Dev. Cell* **24**, 635–648 (2013).
39. C. Ketel *et al*., Neocentromeres form efficiently at multiple possible loci in Candida albicans. *PLoS Genet.* **5**, e1000400 (2009).
40. J. Thakur, K. Sanyal, Efficient neocentromere formation is suppressed by gene conversion to maintain centromere function at native physical chromosomal loci in Candida albicans. *Genome Res.* **23**, 638–652 (2013).
41. K. Nishimura, M. Komiya, T. Hori, T. Itoh, T. Fukagawa, 3D genomic architecture reveals that neocentromeres associate with heterochromatin regions. *J. Cell Biol.* **218**, 134–149 (2019).
42. C. Ellermeier *et al*., RNAi and heterochromatin repress centromeric meiotic recombination. *Proc. Natl. Acad. Sci. U.S.A.* **107**, 8701–8705 (2010).
43. D. P. Locke *et al*., Comparative and demographic analysis of orang-utan genomes. *Nature* **469**, 529–533 (2011).
44. D. Tolomeo *et al*., Epigenetic origin of evolutionary novel centromeres. *Sci. Rep.* **7**, 41980 (2017).
45. M. Ventura *et al*., Evolutionary formation of new centromeres in macaque. *Science* **316**, 243–246 (2007).
46. C. M. Wade *et al*.; Broad Institute Genome Sequencing Platform; Broad Institute Whole Genome Assembly Team,Genome sequence, comparative analysis, and population genetics of the domestic horse. *Science* **326**, 865–867 (2009).
47. S. E. Zanders *et al*., Genome rearrangements and pervasive meiotic drive cause hybrid infertility in fission yeast. *eLife* **3**, e02630 (2014).
48. W. Hu *et al*., A large gene family in fission yeast encodes spore killers that subvert Mendel's law. *eLife* **6**, e26057 (2017).
49. N. L. Nuckolls *et al*., *wtf* genes are prolific dual poison-antidote meiotic drivers. *eLife* **6**, e26033 (2017).